Investigations on the Gust Loading of Flexible Sailplanes

By Dipl.-Ing. Max Hacklinger, Neugilching, Germany.

Presented at the 10th OSTIV Congress, June 1965, South Cerney, England

1. Introduction

The gust loading cases of sailplanes in the existing airworthiness requirements are based on serious simplifications: rigid aircraft, step-or ramp-shaped gust with constant gradient distance and constant alleviation factor. These simplifications are justified for stiff and slow sailplanes. For the high performance sailplane with low natural frequencies, however, the gust encounter is a highly dynamic phenomenon with marked resonancies and it is now generally accepted that the application of the old gust formula has become a mere formality in that case.

An additional complication arises when a flexible wing, loaded by a gust, is restrained against the alleviating vertical motion by a winch towing cable. In this case the pilot has no direct indication of the loading intensity since no correlation exists between the acceleration of the fuselage and the load on the wing.

In a steady winch tow we can prevent overloading simply by application of a weak link calibrated to

$S = G_N (n - 1)$

where G_N = weight of the non-lifting parts of the sailplane

n = limit load factor.

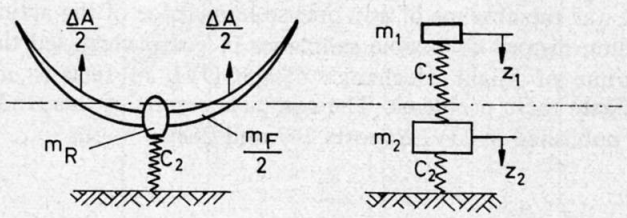

$$(1) \qquad m_1 \ddot{z}_1 = C_1 (z_2 - z_1) - \Delta A$$

$$(2) \qquad m_2 \ddot{z}_2 = C_1 (z_1 - z_2) - C_2 z_2$$

$$(3) \quad \text{with} \quad s = \frac{2vt}{l} \quad \text{and} \quad z' = \frac{dz}{ds}$$

$$(4) \qquad m_1 z_1'' \left(\frac{2v}{l}\right)^2 = C_1 (z_2 - z_1) - \Delta A$$

$$(5) \qquad m_2 z_2'' \left(\frac{2v}{l}\right)^2 = C_1 (z_1 - z_2) - C_2 z_2$$

$$(6) \quad \Delta A = \frac{\rho}{2} v^2 F \frac{dC_A}{d\alpha} \left[\int_0^s \frac{w(s)}{v} \psi (s - \sigma) d\sigma + \frac{2}{l} \int_0^s \Phi (s - \sigma) z_A''(\sigma) d\sigma + \frac{1}{l} z_A''(s) \right]$$

$$(7) \qquad w(s) = \frac{w_0}{2} \left(1 - \cos \frac{\pi s}{s_g}\right) = \text{gust profile}$$

Ψ = Küssner - funktion

Φ = Wagner - funktion

Fig. 1. Dynamic equations of gust problem

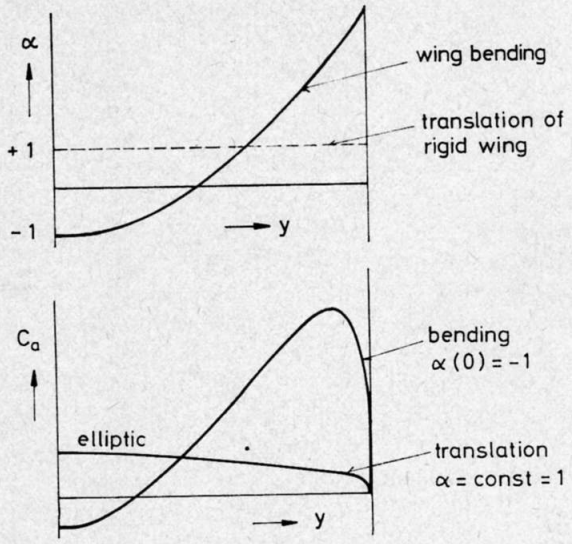

(8) $r = \frac{C_{A\,bd}}{C_{A\,r}} = 2{,}24$ for elliptic distribution of rigid wing.

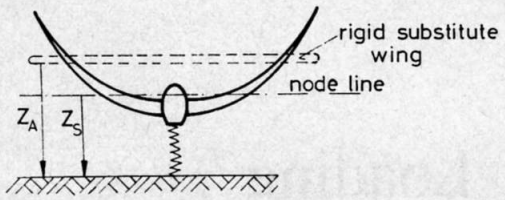

Fig. 2. Equivalent rigid aircraft system

As soon as the motion becomes dynamic, however, this formula no longer applies.

It was the absence of any precise knowledge of the actual loading history of flexible sailplanes in gusts which led the Institute of Flight Mechanics of the DVL in 1960 to investigate these problems. The complete results of this study are published in DVL-reports 267 and 268[1].

2. Propositions

a) From the numerous possible flight configurations we had to select that one which was most important from the gust loading point of view.

It has been shown in the original report that for a given cable strength (or strength of the weak link) the maximum wing load is reached near the end of the tow when the flight path is nearly horizontal. In the altitude region of interest for the sailplane designer, the gust strength increases with altitude. Therefore as initial condition we assume straight, nearly horizontal flight prior to the gust encounter. With this proposition our results are equally valid for the sailplane in tow and in free flight.

b) The atmospheric turbulence is an essentially 3-dimensional phenomenon. But Küssner has shown in the early thirties that in loading cases similar to our sailplane problem the vertical gust component is decisive for the wing loading. Therefore our investigations have been restricted to vertical gusts.

c) The gust distribution over the span is assumed to be uniform. This assumption is conservative for the wing bending strain.

d) We consider two degrees of freedom, viz. vertical translation of the sailplane and wing bending.

e) It is assumed that the wing excited by the gust oscillates in the fundamental bending mode only. Comparative studies with flexible wings of transport aircraft indicate the error due to this assumption to be small.

f) The system of aircraft and cable is reduced to a system of two masses and two springs which retains the kinetic energy, frequency and total mass of the original. Details of this reduction method are given in DVL-report 268.

3. Qualitative Consideration

Before we explain the quantitative analysis we can draw some general qualitative conclusions on the possible loading situations caused by unsteady airloads affecting the sailplane.

If prior to the gust encounter the sailplane has been flown with such high lift that the weak link was fully loaded, then the gust causes the weak link to break immediately and the wing will be relieved. In all other cases, however, part of the airload will be reacted by the fuselage inertia and this produces an additional wing bending moment, the magnitude of which depends on the loading frequency.

(9) $$z_A = z_2 + \frac{1+r}{1+\frac{m_2}{m_1}}(z_1 - z_2)$$

(10) $j = \dfrac{\text{wing root bending moment from gust}}{\text{wing root bending moment in pull up with limit load}}$

$\Delta j =$ increment of load factor due to gust

$$= \frac{\frac{a}{2}(G_N + S_0) + \frac{Bc_1 b/2}{R}\frac{m_1}{m_2}(z_1 - z_2) + \frac{a}{2}\frac{m_1}{R}\left(\ddot{z}_2 + \frac{\ddot{z}_1 - \ddot{z}_2}{1+\frac{m_1}{m_2}}\right)}{\frac{a}{2} n G_N}$$

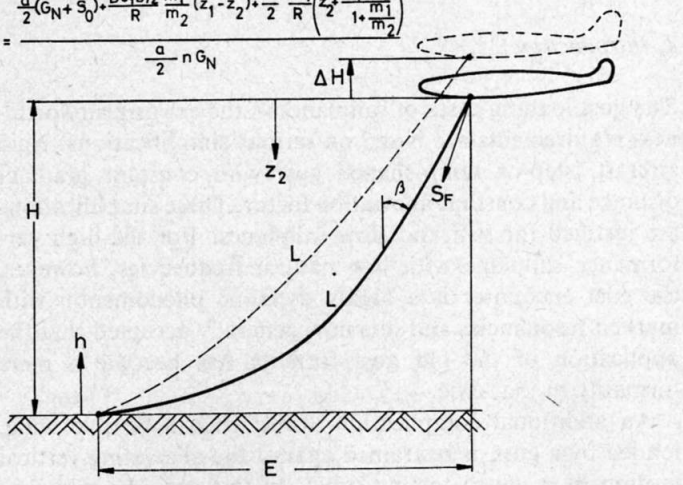

(11) $dS = dl\, K_1 \cos\beta$ $\qquad dh = dl\cos\beta$

(12) $-S d\beta = dl\, D(1{,}1 q \cos^2\beta + K_1 \sin\beta)$ $\qquad de = dl\sin\beta$

(13) $$q = K_2 \left(\frac{h}{H}\right)^2$$

(14) $$C = \left.\frac{\partial S_F}{\partial H}\right|_{\substack{L = \text{const} \\ E = \text{const}}}$$

Fig. 3. Winch towing cable under gravity and aerodynamic forces

[1] M. Hacklinger, A. Pietrass: Untersuchungen über stationäre und instationäre Belastungen von Segelflugzeugen durch Windenschlepp und Böen. DVL-Bericht Nr. 267 (1964)

M. Hacklinger: Ein einfaches Ersatzsystem für die Behandlung von Schwingungsproblemen an Flugzeugen. DVL-Bericht Nr. 268 (1964)

So the steady or quasi-steady methods of load calculation often preferred by designers cannot furnish correct results for free or towed flight in turbulent air. One further effect complicates the situation: By an increase in gust frequency the maximum wing lift is likewise increased.

4. Analysis

a) Motion of the System

In Fig. 1 we have the original aircraft and on the right hand side the substitute system where c_1 represents the wing bending stiffness and c_2 that of the towing cable. Equations (1) and (2) govern the motion of the system. For convenience these equations are transformed by equations (3) from the independent variable time to the nondimensional flight path.

Equation (6) gives the transient lift where w (s) is the gust profile assumed to have a (1 – cosine) shape of variable length, and ψ and φ are the usual approximations for the Küssner and Wagner Functions. Z_A is a representative coordinate yet to be determined from the motion of the substitute system.

In a rigid aircraft, Z_A is equal to the coordinate of the center of gravity, and the additional angle of attack caused by the gust is the same for every wing section, see fig. 2, top diagram. For the wing in bending oscillation, however, we get a second angle of attack distribution corresponding to the wing bending mode. The steady lift distribution for this skewed angle of attack distribution can be calculated by one of several straightforward methods; this is shown in Fig. 2, centre diagram, for an elliptic wing. The spanwise distribution of the unsteady lift does not deviate appreciably from the steady one although the absolute values may be rather different. Now, in our substitute system we suppose the bending wing replaced by a rigid elliptical wing oscillating with the same frequency but with an amplitude such that the integral values of the lift distributions of Fig. 2 become equal. From this condition we have found an amplitude ratio of $r = 2.24$.

With this ratio we can express the "representative coordinate" in terms of the values of the substitute system, as given in Equation (9) of Fig. 3.

b) Loading and reduction method

From the motion of the substitute system we now have to derive the main loading parameter of the sailplane, i. e. the bending moment at the wing root. In order to obtain more general results, we normalize this bending moment with that corresponding to a pull-up to limit load, that quantity which normally determines the design strength of the wing. Equation (10) of Fig. 3 gives the ratio of these two moments which is called "overload factor". $j = 1$ indicates that the limit loading case is reached and $j = 2$ indicates rupture according to the German airworthiness requirements for sailplanes with a safety factor of 2.

The derivation of the expression for j cannot be given in full detail here. The quantities in the final formula for j in Fig. 3 are as follows: S_o is the cable load prior to the gust encounter. B and R are constants for sailplanes with similar mass- and stiffness distributions. B represents an integral

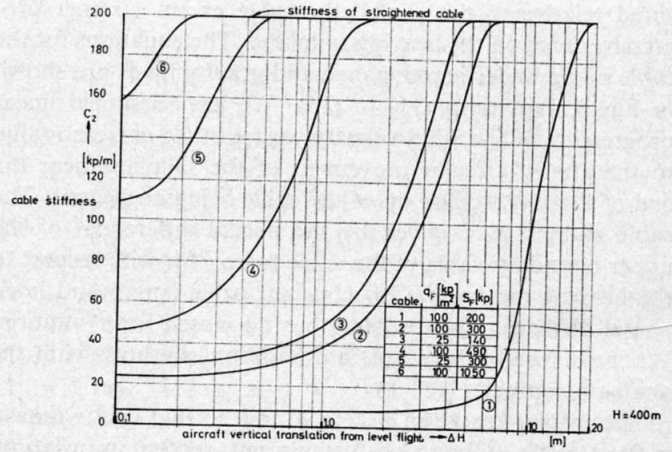

Fig. 4. Cable characteristics for different preloads and wind velocities

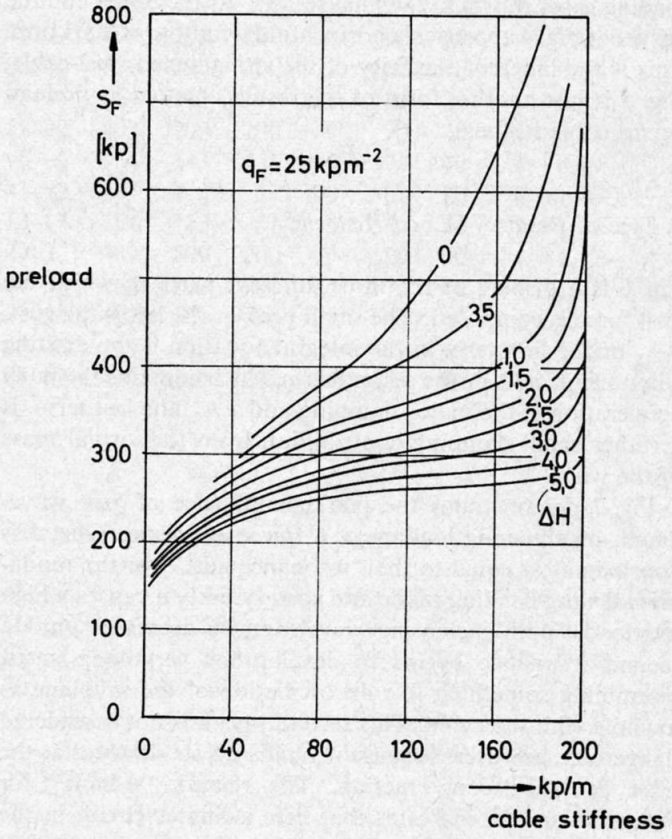

Fig. 5. Cable stiffness and preload

value of generalized mass- and stiffness distributions. In order to obtain a numerical value for B we have measured the fundamental bending mode of a Ka7 sailplane. R is the factor by which the actual wing mass must be reduced to obtain the mass m_1. (The reduction method is given in detail in DVL-report 268.) The last term in Equation (10) containing the system acceleration turns out to be negligibly small. From this we may not, however, conclude that the acceleration terms in the expression for ΔL are likewise negligible, since here they are decisive.

c) Towing Cable

We have to give some comment now on the cable stiffness c_2. Due to the sag of winch towing cables which is usually in the order of 5 to 10% of the cable length (mea-

sured relative to the chord) the cable exerts a rather progressive force on the heaving sailplane. The equations for the cable curve under aerodynamic and gravity loads are shown in Fig. 3, Equations (11) to (13). We have assumed linear progression of the wind velocity with altitude corresponding to the almost circular movement of the sailplane near the end of the tow (rolling up of the cable being neglected). The cable stiffness c_2 is given by the partial differential of the upper boundary value of the cable force ∂S_F with respect to the heaving motion ∂H for constant cable length and horizontal distance. This problem has no closed form solution. We have used, therefore, an iteration method with the analog computer.

The results are given in Fig. 4 and 5. In Fig. 4 we have plotted cable stiffness against aircraft vertical translation. Parameters are dynamic pressure and preload at the upper end of the cable. The cable types 1 to 6 refer to investigated loading cases shown in the final results. At the upper end the curves of Fig. 4 approach a horizontal asymptote of 200 kp/m. This is the inherent elasticity of the straightened steel-cable. Fig. 5 is just another form of the results, plotted as preload versus cable stiffness.

5. *Typical Results of Load Histories*

Fig. 6 is a display of the three different parts of which the gust force is composed. The small peak at the left is the gust. ΔA_1 or the first term in the integral equation is the exciting component, ΔA_2 or the second term which contains the body acceleration is the major damping and ΔA_3, the last term, is a rather small damping contribution from the virtual mass of the wing.

Fig. 7 demonstrates the marked influence of gust wavelength on the wing loading of a towed sailplane. Gust 1 is approximately equal to the "resonance gust" for the fundamental wing bending mode and consequently it causes a high overload. With increasing wavelength, j decreases until a second resonance begins to develop for very long gusts, resembling something like an oscillation of the sailplane as a whole with the cable. This second j-peak is not considered dangerous, however, because it builds up so slowly that the pilot can take counteraction. The remark "α-limit" for curves 11 and 12 indicates that here a limiter circuit in the computer holds the lift at its maximum dynamic value. In practice the sailplane would stall here.

Whereas alterations of the cable characteristics have negligible influence on the first maximum of the load for sailplanes with high wing fundamental frequency, the cable has marked influence on the loading of the low-natural-frequency sailplane, as shown in Fig. 8. The free flying sailplane would experience the first loading peak only, but the restrained sailplane has to suffer a second load which is even higher. In the upper part of Fig. 8 the counter-movement of wing and fuselage mass is plotted versus flight path.

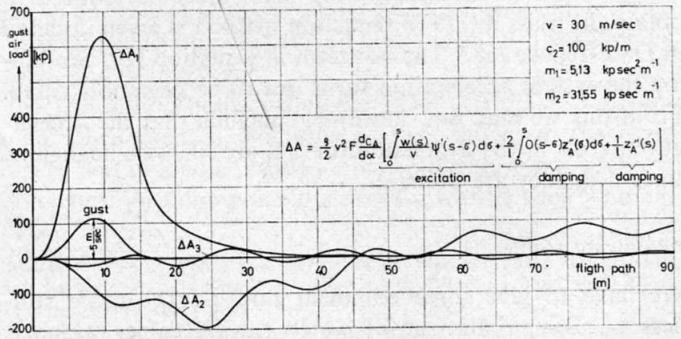

Fig. 6. The three components of the gust airload

6. *Statistics of Loading Cases*

The principal objective of our study was to calculate realistic gust loads in winch tow and free flight conditions for the existing generation of sailplanes and, subsequently, to estimate how far the gust loads would increase if an especially gust-sensitive sailplane were to be constructed within the usual range of design parameters. Table 1 shows the extreme values of the design parameters for certificated German sailplanes. In the dynamic equations of Fig. 1 no direct influence of the design parameter can be detected; therefore we had to cover the whole field of parameter values. From the extremes of Table I and the extreme values for airspeed and cable preload $2^6 = 64$ possible combinations ("cases") can be formed. Some cases could be eliminated with simple reasoning, the rest has been investigated on the computer. For each hypothetical sailplane we have found by iteration that gust length, which caused the highest first peak of the wing load (resonance gust). The results are given in Table II in ascending order of the overload factor, which amounts to as much as 1,96 in one case.

To illustrate the possible gust loading of some actual sailplane designs which had been suspected to give widely different results, we have prepared Table III. It shows that the alarming situation of Table II is not yet realised since in free flight the limit load is not exceeded with a 5 m/sec gust and 30 m/sec flight velocity. But this is not a proof that in a reasonable new design the high values of Table II cannot be reached. It should be noted further that only load factor increments are listed in the tables. In normal winch towing a preload of $j_{st} = 0.5$ to 1.0 is active prior to the gust attack.

Having calculated so many different cases, we had expected to find some correlation between the design parameters and the severity of gust loading, in order to give the designer some rule of thumb. But obviously the gust encounter is of too complex a nature to show such a simple correlation. The only easy deduction from Table III is that decreasing wing stiffness is apt to increase gust loads. Concluding this paragraph on design statistics, it should be mentioned that the analog computer is a very convenient tool for parametric studies; it makes possible rapid calculation of complex gust loading histories and should be used also for the evaluation of unconventional new designs.

7. *Some Remarks on the Gust*

The results of our investigations are based on a harmonic gust of 5 m/sec. We have chosen this value by comparison of the existing gust statistics which indicate that the 5 m/sec gust is likely to be encountered by sailplanes with reasonable frequency. Also we have selected the proper resonance gust length for each sailplane because in our region from 5 to 30 m the turbulence measurements indicate no marked difference in gust frequency.

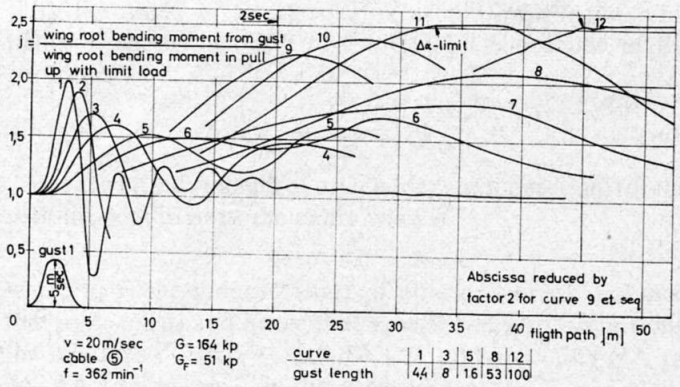

Fig. 7. Influence of gust length on wing loading of towed sailplane

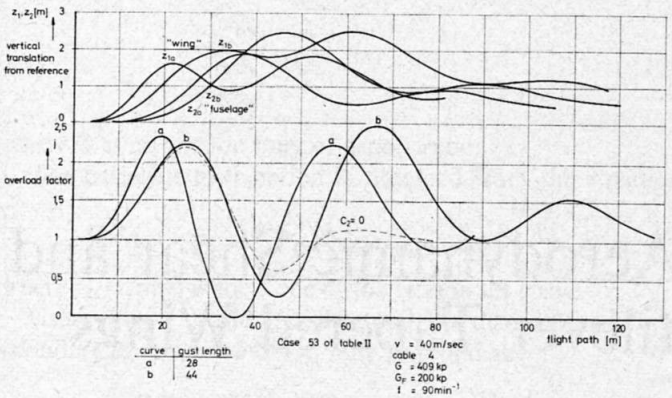

Fig. 8. Gust response of sailplane with heavy wing of small natural frequency

The available data on atmospheric turbulence in the altitude region from 0 to 500 m are insufficient, however, to answer the question how often a sailplane will meet its resonance gust. There is an urgent need for more detailed experimental investigations in this field.

8. Conclusions

The analog computer study of a broad field of actual and possible sailplane designs allowing for wing elasticity and for the presence of the towing cable, has shown that the gust loads can be much higher than indicated by the simple formulae of the airworthiness requirements. There is a marked dependence between gust load and gust wavelength. A weak link in the towing cable serves to limit the steady preload; this weak link is almost useless in limiting the dynamic gust load. Especially for sailplane designs with low fundamental wing bending frequency a more detailed gust analysis is recommended for determining rough air speed and winch towing limitations. This could be combined with the flutter analysis, which is very similar and uses the same aeroelastic derivatives.

Table I

Parameter	*Min.*	*Max.*	*Dim.*
F	9	23	m^2
C_1	500	2200	kp/m
m_1	1,7	6,7	kp sec^2m^{-1}
m_2	(15)	(54)	kp
	15 25	35 54	kp

Table II

case	G *kp*	G_N *kp*	G_F *kp*	F m^2	f min^{-1}	V $\frac{m}{sec}$	sg *m*	Δj	
7– 8	262	211	51	9	169	40	16	0,35	
23 –	596	396	200	9	88	40	31	0,38	
43–44	262	211	51	23	355	20	4	0,40	
15 –	262	211	51	9	355	40	8	0,40	
9 –	164	113	51	9	362	20	4	0,43	α-limit
31–32	596	396	200	9	183	40	14	0,45	
1 –	164	113	51	9	173	20	8	0,46	α-limit
35–36	262	211	51	23	169	20	12	0,49	α-limit
29–40	262	211	51	23	169	40	16	0,54	
55–56	596	396	200	23	88	40	31	0,60	
47–48	262	211	51	23	355	40	8	0,75	
57 –	409	209	200	23	189	20	4,5	0,80	α-limit
49 –	409	209	200	23	90	20	14	0,82	α-limit
63–64	596	396	200	23	183	40	12	0,84	
33–34	164	113	51	23	173	20	8	0,87	
21–22	409	209	200	9	90	40	28	0,93	
5– 6	164	113	51	9	173	40	9	0,99	
41–42	164	113	51	23	362	20	4	1,02	
13–14	164	113	51	9	362	40	7	1,05	
29–30	409	209	200	9	189	40	14	1,12	
37–38	164	113	51	23	173	40	14	1,21	
53–54	409	209	200	23	90	40	28	1,34	
45–46	164	113	51	23	362	40	7	1,78	
61–62	409	209	200	23	189	40	14	1,96	

Table III

case	*sail-plane*	G *kp*	G_N *kp*	G_F *kp*	C_1 kpm^{-1}	f min^{-1}	s_g *m*	Δj^*
65	K 7	480	320	160	2000	202	10	0,63
66	Spatz A, B	220	150	70	586	160	11,6	0,68
67	L-Spatz	250	170	80	499	138	14,2	0,64
70	Ka 6	300	195	105	1335	198	10	0,80
72	Phönix	265	170	95	800	161	12,7	0,87
74	Zugvogel III	365	215	150	1064	148	14,3	0,88
77	Geier I	360	200	160	796	126	15,4	0,96
78	Geier II	370	230	140	1083	155	12,5	0,76
86	Condor IV	520	310	210	1760	162	12,8	0,87
88	Kranich III	520	345	175	2110	192	10	0,68
89	SB 6	350	205	145	400	95	22	0,80